Magazine of Civil Engineering

ISSN 2712-8172

journal homepage: http://engstroy.spbstu.ru/

Research article

UDC 69.07

DOI: 10.34910/MCE.114.1

Shear strengthening of RC beam using RFRP composites

X. Gai , ***D. He*** , ***H. Wang*** ✉

Northeast Forestry University, Harbin, Heilongjiang, China

✉ *wanghongguang@zoho.com*

Keywords: natural fibers, surface treatment, strength of materials, shear stress

Abstract. Partial or complete replacement of non-renewable composite materials with natural fiber reinforced polymer composites, such as basalt fiber, carbon fiber and glass fiber reinforced polymer composite can reduce the consumption of non-renewable resources and damage to the ecological environment in civil engineering construction. It is of great significance for solving global warming, developing green manufacturing and low-carbon cities, and promoting sustainable development in civil engineering. Therefore, this paper focused on mechanical properties of ramie fiber reinforced polymer (RFRP) composites. Futhermore, the shear capacity of RC beams strengthened with ramie fiber sheet was studied, and the bearing characteristics and failure modes of RC beams strengthened with fiber reinforced polymer composites was analyzed. The results show that after the surface treatment with dilute hydrochloric acid, silane coupling agent (KH-550 and KH-560) and aluminum zirconium coupling agent, the mechanical properties of RFRP composites enhanced significantly. Moreover, the surface wettability and interfacial properties of ramie fiber to the epoxy resins were improved by about 40 %. The shear strength results show that after the reinforcement of ramie fiber sheets, the bearing capacity and mid-span deflection of RC beams were greatly improved, and the silane coupling agent (KH-560) modifying ramie fiber sheets had better reinforcement than other fiber sheets. It could be concluded that the replacement of ordinary fiber sheets by ramie fiber sheets can not only reduce the consumption of non-renewable resources, but also improve the shear resistance of RC beams strengthened with the fiber sheets.

Acknowledge: The work was financially supported by the Heilongjiang Natural Science Foundation (Project No. LH2019E112).

Citation: Gai, X., He, D., Wang, H. Shear strengthening of RC beam using RFRP composites. Magazine of Civil Engineering. 2022. 114(6). Article No. 11401. DOI: 10.34910/MCE.114.1

1. Introduction

Material is the material basis for human survival and a pillar industry for the development of the country's national economy. With the continuous development of new technologies and new processes in the field of engineering, higher requirements are imposed on new materials, which not only require excellent mechanical properties and good durability, but also have environmental protection, renewable, and degradable functions [1, 2]. Fiber reinforced composite (FRP) material is a kind of structural material with high strength, low density and excellent design performance [3], which is composed of reinforcing fiber and resin matrix. It has a wide range of applications in machinery, aviation, chemical industry, etc. The fiber in FRP composite material is widely used carbon fiber, glass fiber and basalt fiber, including new high-performance fibers, such as alumina fiber and silicon carbide fiber. With the continuous development of new technologies and new equipment, high-performance fibers make composites materials functionalization and high-performance development.

At present, in the fields of aerospace, transportation, infrastructure construction, energy and environmental protection, high-performance fibers and their FRP composite materials have played an increasingly important role and have become irreplaceable. Basalt fiber has excellent properties such as high strength, high modulus and corrosion resistance [4]. It is an ideal and reinforcing material with no pollution. Ramie fiber has high specific strength, short growth period, environmental friendliness, wide source and low price [5]. Advantages, as reinforcing fiber materials used in civil engineering structures, can be reduced the consumption of non-renewable resources and the destruction of the ecological environment in civil engineering construction are of great significance for solving global warming, developing low-carbon buildings and cities, and promoting the sustainable development of civil engineering.

China is the largest country use concrete in the world. Under the dual action of long-term natural environment and service load, the bearing capacity of the structure gradually decreases. The reliability of the structure will gradually decline, threatening the safety of the use of the structure. In recent years, the application of FRP composite materials in the field of civil engineering reinforcement has been a research hotspot at home and abroad [6–8]. With the continuous development of composite technology, high-strength and high-performance carbon fiber sheets, glass fiber sheets and basalt fiber sheets have been applied in practical engineering. The strength of carbon fiber sheets is the highest among various FRPs, but the carbon fiber elongation (about 1 % to 1.5 %) is smaller than that of glass fiber (about 2 % to 5 %) [9].The confined concrete finally shows sudden brittle failure, and the price of carbon fiber sheets is several times higher than that of glass fiber sheets [10]. So the reinforcement cost is relatively high.

Over the last few years, research works found that natural fiber reinforced polymer composite provide a good alternatives to synthetic fiber composites and it has been accepted as a repairing and strengthening materials for structures in the construction industry [11, 12]. Ramie fiber is derived from the phloem portion of ramie and is a naturally renewable plant fiber. Compared to synthetic fibers, the mechanical properties of ramie fiber monofilaments are relatively low, only one-third to one-quarter of that of glass fibers. At the same time, because the surface of the ramie fiber contains a large amount of hydrophilic hydroxyl groups, the water absorption is large, and the wet heat durability of the composite material is poor, which greatly limits the application potential of the ramie fiber as a reinforcing material in the field of civil engineering. At present, the modification methods of ramie fiber surface are mainly treatment [13, 14], ultrasonic treatment [15, 16], chemical coating modification [17–19] and coupling agent modification [20, 21]. These methods only have mechanical properties or interfacial adhesion to ramie fiber monofilament from a single angle [22–24]. The performance of the modification study, without considering the synergistic enhancement of mechanical and interfacial adhesion properties, the modification effect and application prospects are not ideal.

In this paper, the shear capacity, the bearing characteristics and failure modes of RC beams and the RC beams strengthened with ramie fiber sheets, unidirectional basalt fiber sheets by contrast test were studied.

2. Materials and methods

2.1. Materials

(1) Concrete

RC test beam with commercial concrete (concrete grade is C30), water-cement ratio is 0.42, the ratio is cement : water : sand : gravel = 360 : 151 : 632 : 1282. The cement adopts the Swan brand P.O grade 42.5 ordinary Portland cement produced by Harbin Cement Factory of Jilin Yatai Group of China. The maximum particle size of coarse aggregate is about 25 mm. The measured concrete slump is 43 mm. After the pouring is completed, the RC test beam is continuously subjected to room temperature watering for 7 days, and then remove the mold and rinse it to 28 days. The concrete cube compressive strength test was prepared in the same batch after pouring RC test beams, and place it in a standard maintenance room for maintenance 28 days. According to the requirements of the national standard for the test of mechanical properties of ordinary concrete (GB/T 50081-2011), the compressive strength of the concrete cube was measured to be 35 MPa to 40 MPa.

(2) Reinforcement

The longitudinal reinforcement, structural reinforcement and standing reinforcement are respectively 25 mm,14 mm and 12 mm, using HRB400 grade ordinary hot rolled ribbed steel bar. The diameter of the stirrup is 8 mm, using HPB300 grade hot rolled round bar.

According to the requirements of the national standard test method for tensile testing of metallic materials (GB/T 228-2010), the mechanical properties of the steel bars measured are shown in Table 1.

Table 1. Mechanical properties of reinforcements in the RC beams

Rebar type	Reinforcement grade	Diameter (mm)	Yield Strength (MPa)	Tensile strength (MPa)	Elongation (%)
Vertical reinforcement	HRB400	25	410	570	20.0
Structural reinforcement	HRB400	14	410	565	21.5
Erecting steel bars	HRB400	12	390	560	20.0
Stirrup	HPB300	8	310	450	25.0

(3) Ramie fiber sheets and basalt fiber sheets

In order to study on the effect of ramie fiber sheet on the shear resistance of RC beams in different directions and compositions, the preparation of ramie fiber composite material by using two-way ramie fiber sheets produced by China Harbin Linum Textile Co., Ltd. The density of the fiber cloth is 1.5g/cm^3, nominal thickness is 0.16 mm, the spinning process is ring spinning.

In order to compare the effects of different types of ramie fiber sheets on the shear reinforcement of RC beams, this paper also uses basalt fiber sheets to reinforce the RC beams. Basalt fiber sheets is produced by Sichuan Aerospace Tuoxin Basalt Industrial Co., Ltd.

(4) Epoxy resin and curing agent

Attach ramie fiber sheets to the outer surface of RC beams, making it work with RC. The epoxy resin impregnating rubber JZ-A and the curing agent JZ-B are mixed according to a mass ratio of 100:34.5, and cured at room temperature. Measured in the laboratory, the tensile strength and modulus of the epoxy resin impregnated rubber are 59.1 MPa and 3.08 GPa, the glass transition temperature is about 62.5 °C.

2.2. Main instruments and equipment

In the test of shear capacity of RC beams strengthened with ramie fiber sheets, the main test instruments and equipment used are shown in Table 2.

Table 2. Main experimental instruments and equipment

Test instrument and equipment	Specifications and models	Manufacturer
High-speed static strain test analysis system	16 aisle，DH3820	Jiangsu Donghua Testing Technology Co., Ltd.
Pressure Sensor	250t，GD-250T	Fuzhou Jingkong Automation Equipment Co., Ltd.
Linear variable differential transformer	25 mm，MHR-25	Shanghai Ruihong Testing Technology Co., Ltd.
Resistance strain gauge	120Ω, BE120-10AA 120Ω, BQ120-60AA	AVIC Electric Instrument Co., Ltd.

2.3. Experimental program

2.3.1. Structural design of RC beams

Comparative test on shear reinforcement of RC beams with ordinary ramie fiber sheets and basalt fiber sheets. The RC beam has a length of 1800 mm and a section size of 200 mm × 400 mm, and the main structural dimensions are shown in Fig. 1.

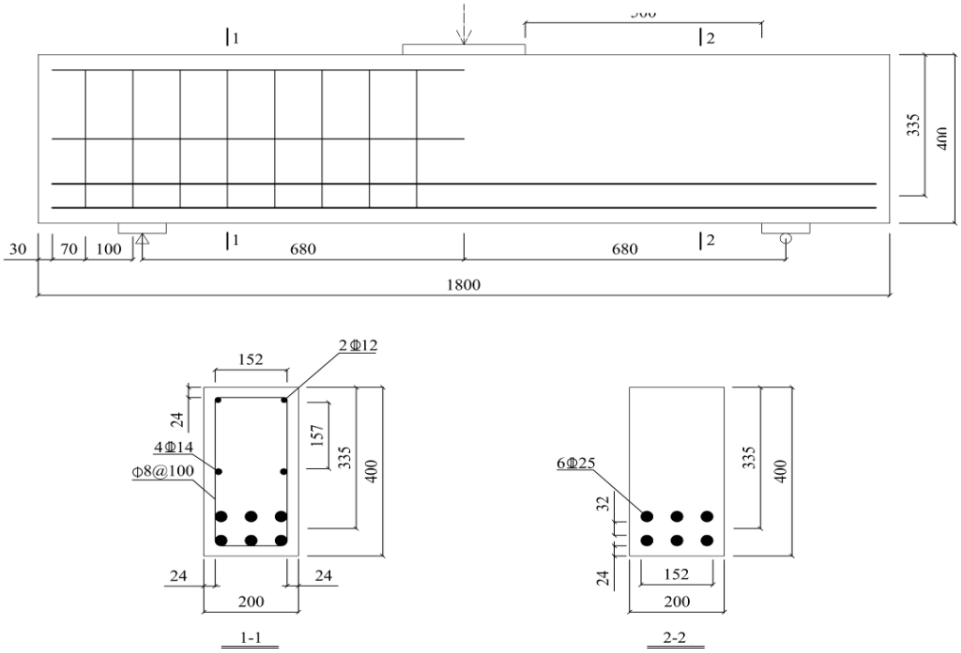

Figure 1. Structural design of the RC beam.

According to the requirements of the national standard of Concrete Structure Design Code (GB 50010-2010), in order to cause shear failure of RC beams, a sufficient number of longitudinal steel bars should be placed in the span of the beams to ensure that the bending failure does not occur before the shear failure. As shown in Fig. 1, the RC beams are equipped with a certain number of stirrups in the left half span, and half-span structural steel bars are arranged in the middle of the cross section to improve the shear capacity of the left half span. At the same time, ensuring the shear failure occurs only in the right half span to facilitate test measurements.

2.3.2. Experimental program of FRP strengthened RC beams in shear capacity

This paper designs 6 RC beams, RC-control is not reinforced, RC-FRP 1 to RC-FRP4 are reinforced with ordinary ramie fiber sheets, and the number of layers is 3 and 6 respectively, the main direction of the ramie fiber sheets is the warp and weft directions. The main direction of the ramie fiber sheets is the warp direction. RC-FRP 5 is reinforced with unidirectional basalt fiber sheets and the number of layers is 1 layer. The experimental program of FRP strengthened RC beams in shear capacity is shown in Table 3.

Table 3. Experimental program of FRP strengthened RC beams in shear capacity

RC beam	Fiber sheets type	Main direction of force	Paste layer
RC-FRP1	Ordinary fiber sheets	vertical	3
RC-FRP2	Ordinary fiber sheets	vertical	3
RC-FRP3	Ordinary fiber sheets	Latitude	6
RC-FRP4	Ordinary fiber sheets	Latitude	6
RC-FRP5	Unidirectional basalt fiber sheets	–	1

The width of fiber sheets is 300 mm and the length of fiber sheets is 1000 mm. Paste mode is U-shaped reinforcement. The paste position is shown in Fig. 2. After the RC beam is finished, transporting it to the experimental site for loading test. In order to facilitate the centering and crack width measurement and recording of the concrete beam loading device and describing the test phenomenon, the side of the RC-control is painted, and the extension direction is divided into 100 mm ×100 mm standard grid. During the test, the three-point bending load is applied and loaded by force. The support mode is the left fixed hinge support and the right movable hinge support. The LVDT sensor is arranged in the span of the RC beam, on the side of the bonded fiber sheets and at the fulcrum, collecteing the longitudinal displacement of the beam at different positions. A resistance strain gauge is attached to the surface of the RC-control concrete surface and the fiber sheets surface of the remaining beams to collect the strain generated by the concrete and the fiber sheets. All displacement and strain signals in the test are converted into potential signals by the strain collector.

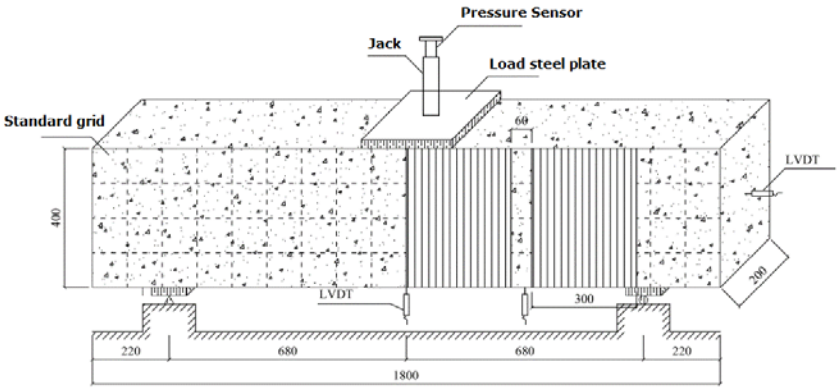

Figure 2. Experimental program of FRP strengthened RC beams in shear capacity.

3. Results and Discussion

3.1. Experimental results and analysis of ordinary RC beams in shear capacity

3.1.1. Major damage phenomena and processes

After 28 days of standard maintenance of all reinforced concrete, transfer it to the test site and attach the fiber cloth according to the experimental program of FRP strengthened RC beams in shear capacity. Firstly, the shear capacity test of RC-control was performed. Before the test, in order to facilitate the centering and crack width measurement and recording of the concrete beam loading device and describing the test phenomenon, the side of the RC-control is painted, and the extension direction is divided into 100 mm × 100 mm standard grid. The mesh and strain gauge placement of the RC-control is shown in Fig. 3.

Figure 3. Mesh and strain gauges on the surface of the RC-control beam.

At the beginning of the test, RC-control produces vertical micro cracks near the beam's span, and there are also many tiny cracks perpendicular to the lower edge of the concrete beam in the unformed stirrups on the right side. As the load continues to increase, the number of right half-span cracks of the beam gradually increases and extends upward. It can be clearly seen that one of the many oblique cracks has the largest width and gradually forms a critical oblique crack. After the occurrence of critical oblique cracks, the number of vertical cracks at the bottom of the mid-span section tends to be stable, and the crack width increases slowly. When the oblique crack expands to a certain extent, the oblique crack begins to branch near the bottom side of the beam, that is, a gentle steel bond crack occurs. As the load increases, the critical oblique crack continues to develop upward and extends below the mid-span loading point. No new oblique cracks will occur until the concrete in the span is crushed and destroyed. RC-control is a typical shear failure mode, and its failure mode and crack distribution are shown in Fig. 4.

Figure 4. Failure modes and crack distribution of RC-control beam.

3.1.2. Characteristic load and load-span displacement curve

Central deflection and load curves of RC-control is shown in Fig. 5. Central deflection and load curves of RC-control is divided into three main stress processes: elastic phase, cracked working phase and critical failure phase. At the beginning of loading, as the load is gradually increased, the mid-span deflection value of RC-control increases linearly.

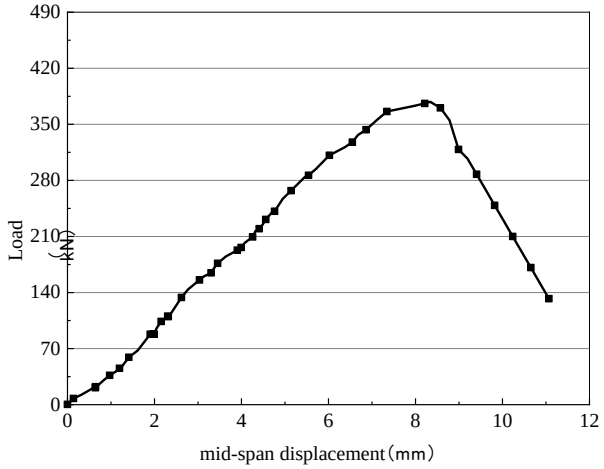

Figure 5. Central deflection and load curves of RC-control beam.

When the load reaches about 176 kN (46.6 %), a crack with the largest width can be found in the right half span of the beam, and a critical oblique crack is gradually formed. When the load reaches 352 kN (93.1 %), the critical oblique crack extends below the mid-span loading point, after which no new oblique cracks appear until the concrete in the span is crushed and destroyed. Finally, the ultimate bearing capacity of the RC-control is 378 kN, and the mid-span ultimate deflection is 8.3 mm.

3.2. Experimental results and analysis of FRP strengthened RC beams in shear capacity

3.2.1. Major damage phenomena and processes

(1) RC beam reinforced with ramie fiber sheets

When the RC beam reinforced with ramie fiber sheets, at the beginning of the loading, no obvious oblique cracks were observed on the RC surface. As the RC beam is subjected to increasing loads, the ramie fiber sheets occasionally makes a slight sound, but no visible damage is seen from the appearance. After that, the load continued to increase, and the RC beam continued to emit a slight crack, and the ramie fiber sheets near the support showed clear cracks in the middle and lower parts, and continued to expand. As the load continued to increase, the ramie fiber sheets suddenly burst into a crisper sound. According to the different reinforcement methods, the load level at this time is 470 kN ~ 495 kN, and the mid-span deflection value is 9.7 mm ~ 10.1 mm. Finally, along with the crisp and loud cracking sound, the ramie fiber sheets near the loading point of the mid-span also exits the work, showing obvious delamination and bulging outward. The concrete in the middle of the span is rapidly crushed, and the RC beam is broken by compression shearing. At the same time, a thin layer of concrete is attached to the inside of the ramie fiber sheets. The failure mode of RC beams strengthened with ramie fiber sheets is shown in Fig. 6.

(2) RC beam reinforced with unidirectional basalt fiber sheets

In order to compare the effect of reinforcing RC with ramie fiber sheets, basalt fiber sheets reinforcement is used as a comparison. At the beginning of the test, no obvious cracks were observed on the surface of the RC beam tension zone. As the load continues to increase, the RC beam is placed on one side of the stirrup first with obvious oblique cracks, and gradually expands and deepens. When the load is increased to about 484 kN, the concrete beam suddenly has a large cracking sound, and the concrete at the bottom of the left beam is peeled off. The reinforcement of the tension zone has reached the yield strength, and the concrete in the compression zone is crushed. The increase of the bearing capacity of the beam is obviously slowed down. When the load reached 543 kN, the reinforced concrete beam suddenly broke. Different from the failure mode of RC beams strengthened with ramie fiber sheets, the basalt fiber sheets did not appear to be broken or peeled off. Finally, the shear capacity of concrete beams is close to the test results of ramie fiber sheets reinforced. The failure mode of RC beams strengthened with basalt fiber sheets is shown in Fig. 6.

Figure 6. Failure mode of the RC beam strengthened with basalt fiber sheets.

3.2.2. Characteristic load and load-span displacement curve

The characteristic loads of RC beams are shown in Table 4.

Table 4. Characteristics load of the RC beams

Numbering	P_1 (kN)	δ_1 (mm)	P_2 (kN)	δ_2 (mm)	P_u (kN)	δ_u (mm)	P_1/P_u (%)	P_2/P_u (%)	ΔP_u (%)
RC-control	–	–	–	–	378	8.3	–	–	–
RC-FRP1	470	9.7	519	10.5	550	11.6	85.6	94.5	45.4
RC-FRP2	488	10.1	528	11.2	565	12.2	86.2	93.3	49.6
RC-FRP3	495	10.1	551	11.1	579	12.3	85.4	95.1	53.2
RC-FRP4	473	10.0	535	11.2	559	11.8	84.7	95.8	47.8
RC-FRP5	–	–	–	–	543	11.7	–	–	43.5

Since the concrete crack in the tension zone cannot be observed after the ramie fiber sheets is reinforced, the cracking load of the concrete is not listed in the table. In Table 4, P_u is the maximum load that the RC beam is subjected to when it is destroyed, that is, the ultimate load value of the beam. P_1 and P_2 are the load values of the first and second ramie fiber sheets of the RC beam when they exit the work, respectively. δ and δ_u are the measured deflection and ultimate deflection of the RC beam. δP_u is the RC after reinforced with ramie fiber sheets, the shear capacity increase percentage of RC.

Characteristics load of the RC beams was shown in Table 4. It can be seen that the ultimate bearing capacity of the beam without reinforcement is 378 kN, and the value of the mid-span deflection is 8.3 mm. When the RC beam is reinforced with ramie fiber sheets, the bearing capacity level is significantly improved. After reinforcement by ordinary ramie fiber sheets, the bearing capacity of the beam reaches 550 kN ~ 579 kN, which is 45.4 % ~ 53.2 % higher than that of the unreinforced beam. Among them, the shear capacity of the beams strengthened with three layers of radial ordinary ramie fiber sheets are 550 kN and 560 kN, respectively, and the mid-span ultimate deflection values are 11.6 mm and 12.2 mm respectively.

While the 6-layer latitudinal ordinary ramie fiber sheets is used to reinforce the beam, the shear capacity of the beams are 579 kN and 559 kN, respectively, and the mid-span ultimate deflection values are 12.3 mm and 11.8 mm, respectively. The test results of the above four RC beams are relatively close. When reinforced with 1 layer of unidirectional basalt fiber sheets, the shear capacity of RC beam is 543 kN, and the mid-span ultimate deflection value is 14.6 mm. The shear reinforcement effect of RC beam is similar to that of ordinary ramie fiber sheets, moreover, the shear capacity of RC beams strengthened with ramie fibers sheets is higher than that of RC beams reinforced with basalt fibers sheets.

The load-span displacement curve of RC beams strengthened with ramie fiber sheets and basalt fiber sheets are shown in Fig. 7. It can be seen that the ramie fiber sheets can significantly improve the shear capacity of the RC beam, and the development trend of the load-span displacement curve under different reinforcement schemes is relatively close. When the load is small, the mid-span displacement value of the RC beam increases slowly. When the ramie fiber sheets is subjected to an increasingly large external force, the growth of the mid-span displacement of the concrete gradually slows down, indicating that the stress redistribution process is taking place inside the concrete.

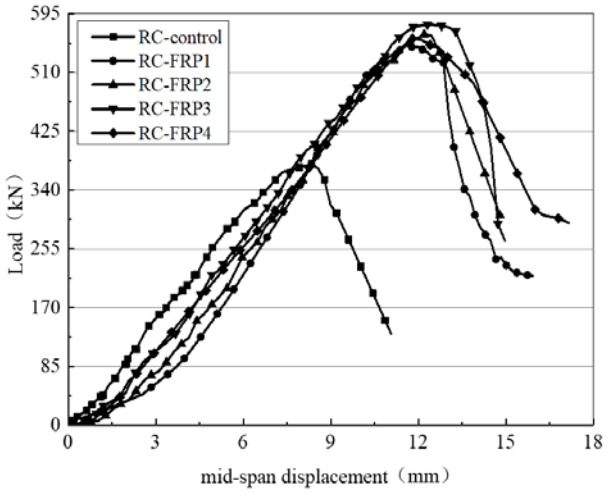

Figure 7. Central deflection and load curves of the RC beam strengthened with fiber sheets.

The test results show that, on the one hand, ramie fiber sheets can effectively enhance the shear resistance of RC beams and improve the shear capacity of concrete beams. The effectiveness of structural reinforcement has been verified. On the other hand, the ductility of the concrete beam is improved, and the resistance of the concrete beam to deformation is enhanced. Therefore, RC beams reinforced with ramie fiber sheets not only meet the bearing capacity requirements, but also meet the structural ductility requirements.

3.2.3. Strain distribution of ramie fiber sheets

As a comparative test beam, 10 sets of resistance strain gauges were placed on the right side of the unplaced stirrups, and the pasting positions and numbers are shown in Fig. 8. All the resistance strain gauges are attached to both sides of the main oblique crack, which can accurately detect the strain change generated when the concrete beam cracks.

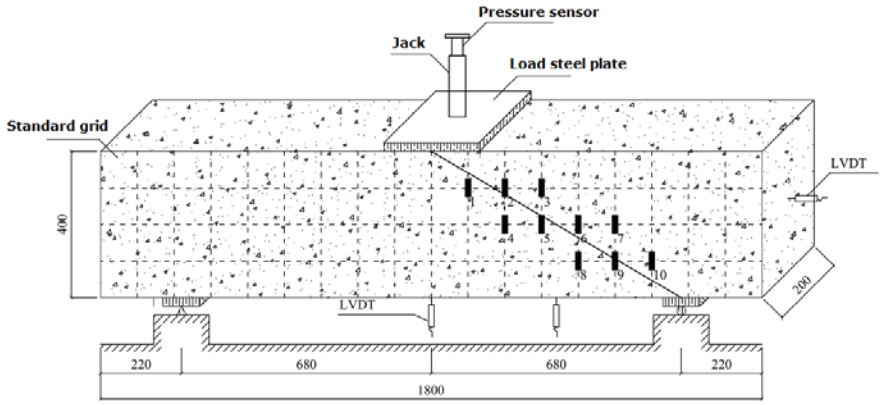

Figure 8. Strain gauges on the RC-control beam.

Taking the mid-plane of the concrete beam as the reference plane, dividing 10 resistance strain gauges into three groups, the first group (numbered 1, 2, and 3), the second group (numbered 4, 5, 6, and 7) and the third group (numbered 8, 9, and 10). Each set of resistance strain gauges collected load levels of 50 kN (13.2 %), 150 kN (39.7 %), 220 kN (58.2 %), 300 kN (79.4 %) and 350 kN (92.6 %) as representative measurement points. The strain distribution of each resistance strain gauge is shown in Fig. 8 (the abscissa number in the figure is the corresponding resistance strain gauge number).

It can be seen from Fig. 9 that as the load level is gradually increased, part of the resistance strain gauges are out of operation due to excessive deformation, so some data points in the figure are missing. The oblique crack of ordinary reinforced concrete beam is gradually developed from the support to the oblique upward. With the gradual increase of the load, the direction of the main oblique crack may appear in Fig. 6, and a major oblique crack is formed in several oblique cracks called critical oblique crack.

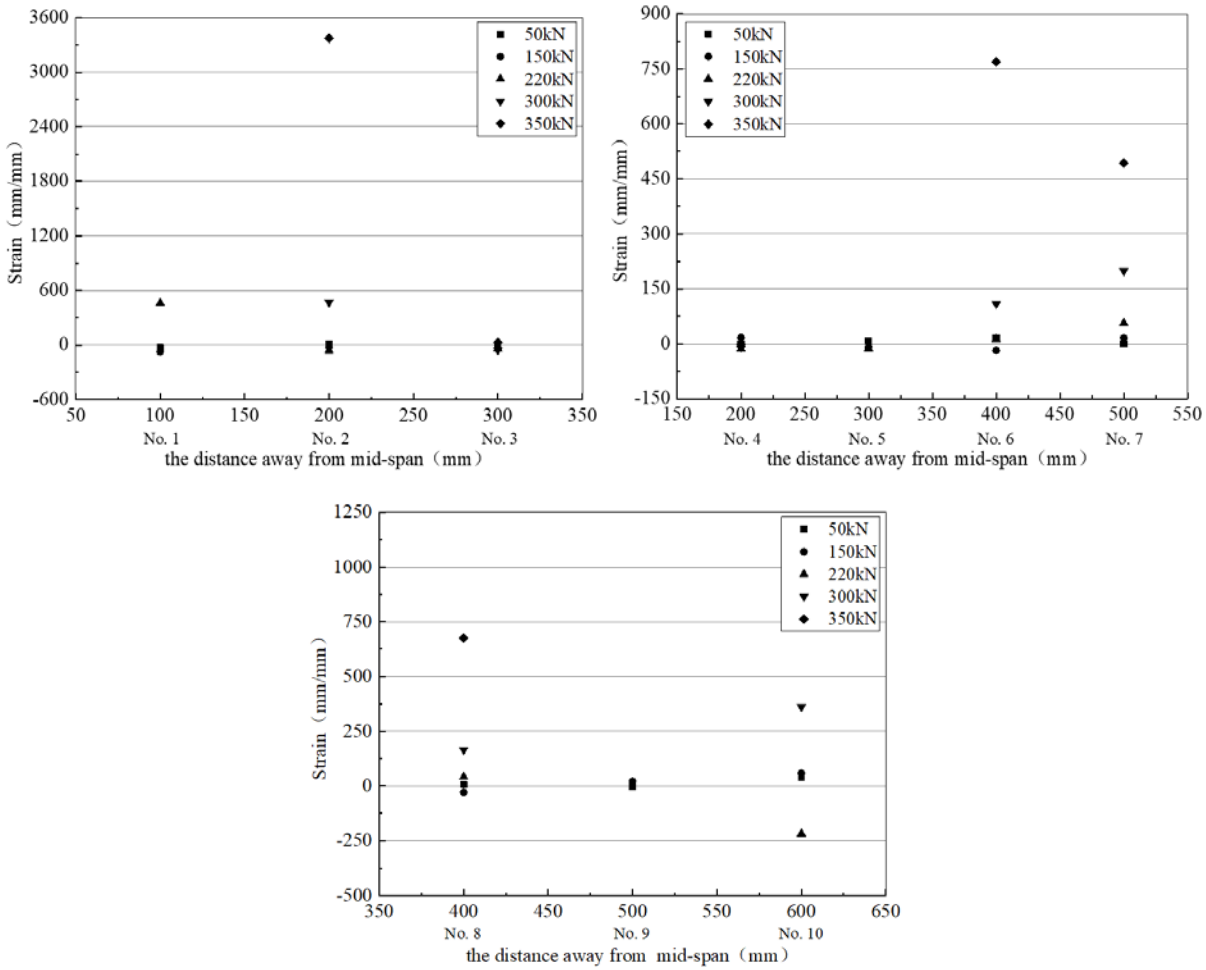

Figure 9. Strain distribution of concrete for RC-control beam.

According to the curve in Fig. 9, it can be found that the development of the oblique crack of the ordinary RC beam has passed through the 8th, 6th and 2nd resistance strain gauges. After the critical oblique crack occurs, the beam can continue to bear the load until the stirrup intersecting the oblique crack reaches the yield strength, and the concrete in the shear zone is crushed. At the same time, the concrete at the uppermost shearing zone of the oblique crack reaches the ultimate strength under the combined action of shear stress and compressive stress, and the steel and coagulation are fully utilized, similar to the normal section of the reinforced failure. However, compared with the normal section failure of the beam, the damage is sudden and belongs to brittle failure. Since the shear span ratio of the reinforced concrete beams prepared in this paper is between 1 and 3, the damage of the reinforced concrete beams is a typical shear failure.

Unlike the ordinary RC beams, after reinforcement with ramie fiber sheets, most of the surface of the concrete beam is covered and does not have the conditions for determining the strain of the concrete. Therefore, in this paper, the same type of 10 resistance strain gauges are attached to the surface of the ramie fiber sheets of each RC beam to measure the strain distribution of the ramie fiber sheets. The position and number of the resistance strain gauges of the RC beams are shown in Fig. 8.

All the resistance strain gauges are attached to both sides of the main oblique crack, which can accurately detect the cracking of the RC and cause the strain change of the ramie fiber sheets. The same as the strain distribution on the concrete surface, when calculating the strain distribution of the ramie fiber sheets, the 10 resistance strain gauges are divided into three groups. The first group (numbered 1, 2, and 3), the second group (numbered 4, 5, 6, and 7) and the third group (numbered 8, 9, and 10). At the same time, the resistance values generated by the respective strain gauges as the load is gradually increased are collected.

Each set of resistance strain gauges collected load levels of 15 %, 40 %, 60 %, 80 %, and 95 % as representative measurement points. The strain distribution of each of the resistance strain gauges of RC-FRP2, RC-FRP4, and RC-FRP5 is as shown in Fig. 10 to 12 (the abscissa number in the figure is the corresponding resistance strain gauge number).

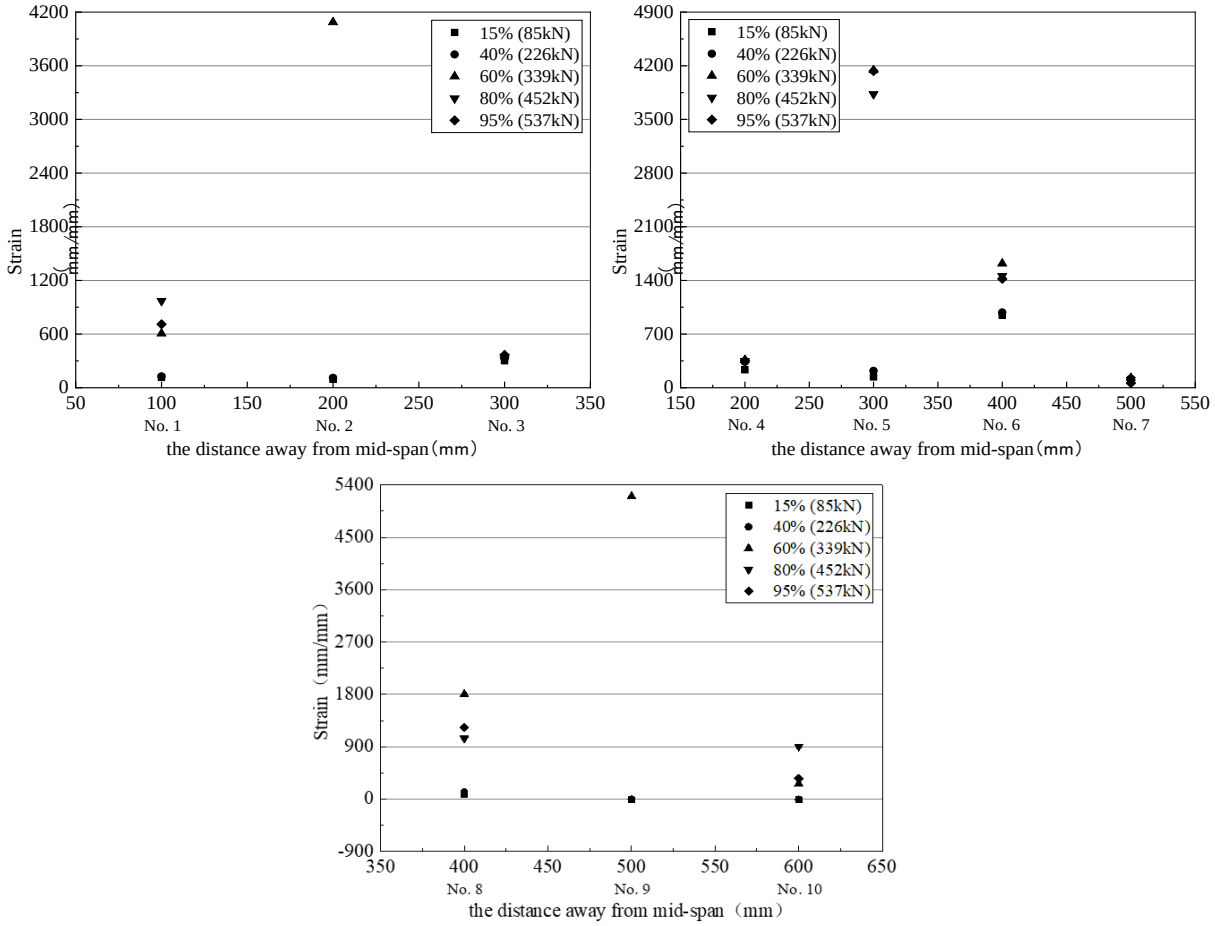

Figure 10. Strain distribution of flax fiber sheets for the RC-FRP2 beam.

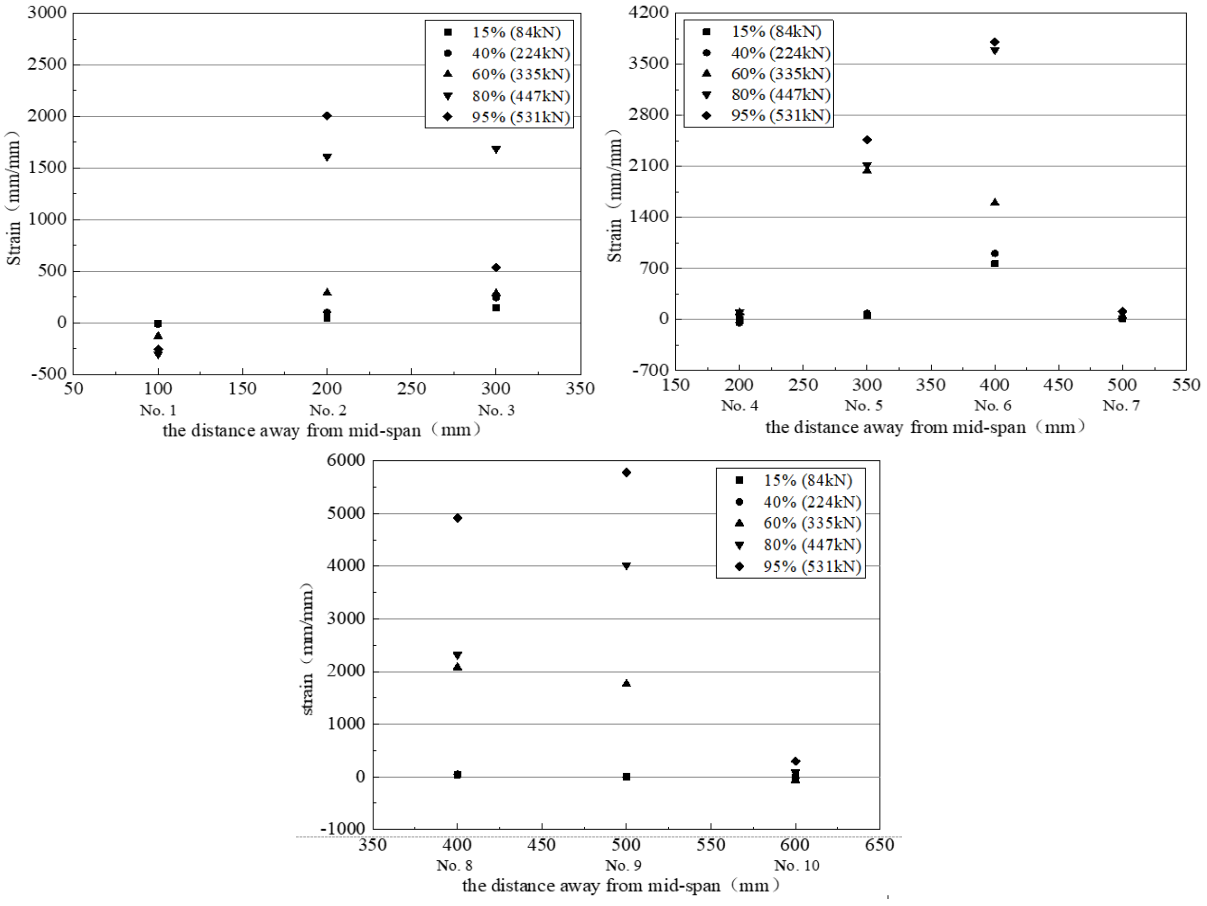

Figure 11. Strain distribution of flax fiber sheets for the RC-FRP4 beam.

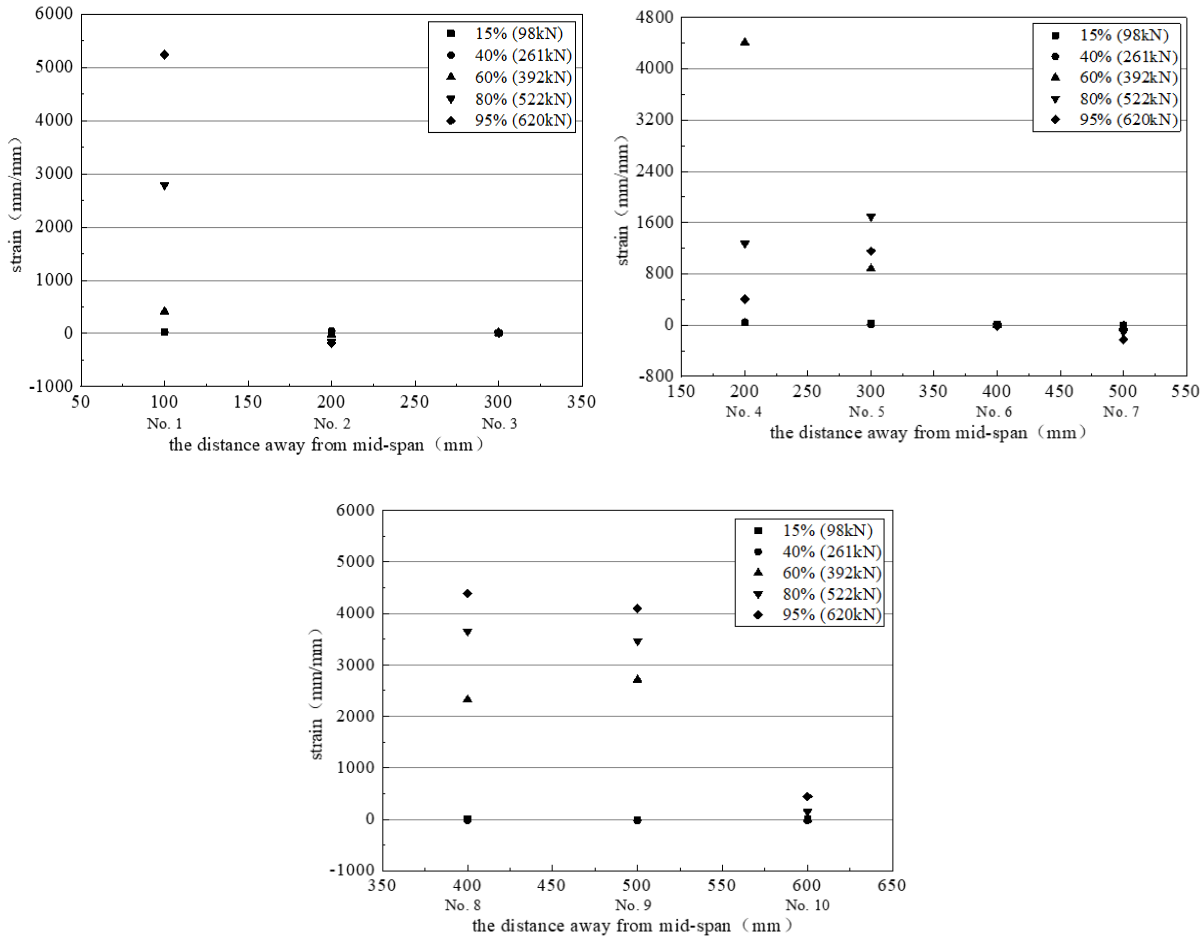

Figure 12. Strain distribution of flax fiber sheets for the RC-FRP5 beam.

It can be seen that the strain distribution of the ramie fiber sheets has a certain regularity. When the load level is low, that is, before the cracking of the RC beam occurs, the strain of the fiber cloth is small, this indicates that the ramie fiber sheets has not yet assumed sufficient external force. As the load level gradually increases, the RC beam gradually approaches the cracking load, and the strain value of the ramie fiber sheets suddenly increases, indicating that the ramie fiber sheets attached to the side of the concrete beam begins to function (the 60 % horizontal curve in Fig. 10 to 12).

At this stage, the ramie fiber sheets shown the same effect as the other side stirrup, and as the load level is gradually increased, the load on the ramie fiber sheets is gradually increased, and the generated strain value is gradually increased.

As shown in Fig. 8, the main oblique crack of the RC beam passes through the strain gauges No. 9, No. 6, No. 5 and No. 2 in sequence. Therefore, as the load level is gradually increased, the above-mentioned resistance strain gauge gradually withdraws from the working state. The cracking of the concrete oblique section causes the concrete to basically withdraw from the work, so the contribution to the shear performance is low. At this time, the shear capacity is mainly provided by the ramie fiber sheets, and he ramie fiber sheets has the largest strain in the middle of the beam.

As can be seen from Fig. 10 to 12, the ramie fiber sheets near the crack has a larger strain value and the strain value away from the crack is smaller. The main reason is that the peeling of the ramie fiber sheets is gradually extended from the crack to the upper and lower free ends. At the same time, the failure mode of RC beams strengthened with ramie fiber sheets indicates that the fracture failure of the ramie fiber sheets occurs before the peeling damage of the ramie fiber sheets and concrete interface, which is due to the low tensile strength of the ramie fiber sheets. According to the existing research results, the effect of the fiber cloth attached to the longitudinal direction of the concrete beam on the shear capacity of the beam is not obvious, however, the ramie fiber sheets attached to the side of the concrete beam at other angles can improve the shear capacity of the concrete beam [25]. Therefore, the arrangement of the main force direction of the ramie fiber sheets should form a certain angle with the oblique crack of the reinforced concrete, which is beneficial to the performance of the ramie fiber sheets, and has strong engineering feasibility and economic rationality.

4. Conclusion

This paper using the ramie fiber sheets to strengthen the shear capacity of the RC beams and investigating the bearing characteristics and failure behavior of the strengthened RC beams were. After that, the shear capacity formula for the RC beams strengthened by the ramie fiber sheets was put forward. The main conclusions of the research are as follows:

(1) Compared with unreinforced RC beams, the shear capacity and mid-span deflection of RC strengthened with ramie fiber sheets fabrics have been greatly improved. After reinforcement of ordinary ramie fiber sheets, the shear capacity of RC beams is 550 kN ~ 579 kN, which is 45.4 % ~ 53.2 % higher than that of unreinforced RC beams. At the same time, the beam's mid-range deflection reached 11.6 mm ~ 12.3 mm, which were 39.8 % ~ 48.2 % higher than that of unreinforced RC beams.

(2) Through the results of the shear capacity, it can be concluded that the shear capacity and mid-span deflection of RC beams strengthened with ramie fiber sheets are higher than those of basalt fiber sheets. Moreover, the main producing area of ramie fiber is Heilongjiang Province, accounting for 80 % of the country's ramie fiber planting area, and the price is cheap. The use of ramie fiber sheets instead of non-renewable composite materials can reduce the consumption of non-renewable resources and damage to the ecological environment in civil engineering construction, solve global warming, develop green manufacturing and low-carbon cities, and promote the sustainability of civil engineering has a great significance.

(3) Taking the ultimate strain of ramie fiber sheets as a control index, the shear capacity of RC beams after reinforcement has a good linear relationship with the cuff ratio of ramie fiber sheets. The calculation formula of shear capacity of RC beams strengthened with ramie fiber sheets reinforced by ordinary ramie fiber sheets was preliminarily proposed by curve fitting.

References

1. Teng, J.G., Yu, T., Fernando, D. Strengthening of Steel Structures with Fiber-Reinforced Polymer Composites. Journal of Constructional Steel Research. 2012. No. 78. Pp. 131–43. http://dx.doi.org/10.1016/j.jcsr.2012.06.011
2. Ramesh, M. Flax (Linum Usitatissimum L.) Fibre Reinforced Polymer Composite Materials: A Review on Preparation, Properties and Prospects. Progress in Materials Science. 2019. No. 102. Pp. 109–66. http://dx.doi.org/10.1016/j.pmatsci.20-18.12.004
3. El-Enein, H.A., Azimi, H., Sennah, K., Ghrib, F. Flexural Strengthening of Reinforced Concrete Slab-Column Connection Using CFRP Sheets. Construction and Building Materials. 2014. No. 57. Pp. 126–137. http://dx.doi.org/10.1016/j.conbuildmat.2014.01.077
4. Sateshkumar, S.K., Awoyera, P.O., Kandasamy, T., Nagaraj, S., Murugesan, P., Ponnusamy, B. Impact Resistance of High Strength Chopped Basalt Fibre-Reinforced Concrete. Revista De La Construccion. 2018. No. 17, no. 2. Pp. 240–248. http://dx.doi.org/10.7764/rdlc.17.2.240
5. Wang, X.M. Petru, M. Effect of Hygrothermal Aging and Surface Treatment on the Dynamic Mechanical Behavior of Flax Fiber Reinforced Composites. Materials. 2019. No. 12, no. 15. Pp. 10. http://dx.doi.org/10.3390/ma12152376
6. Mahmoudi, S., Kervoelen, A., Robin, G., Duigou, L., Daya, E.M., Cadou, J.M. Experimental and Numerical Investigation of the Damping of Flax-Epoxy Composite Plates. Composite Structures. 2019. No. 208. Pp. 426–33. http://dx.doi.org/10.1016/j.compstruct.2018.10.030
7. Li, Yeou-Fong, Ming-Jer Tsai, Ting-Fang Wei, Wei-Chou Wang. A Study on Wood Beams Strengthened by FRP Composite Materials. Construction and Building Materials. 2014. No. 62. Pp. 118–25. http://dx.doi.org/10.1016/j.conbuildmat.2014.03.036
8. Chroscielewski, J., Ferenc, T., Mikulski, T., Miskiewicz, M., Pyrzowski, L. Numerical Modeling and Experimental Validation of Full-Scale Segment to Support Design of Novel GFRP Footbridge. Composite Structures. 2019. No. 213. Pp. 299–307. http://dx.doi.org/10.1016/j.compstruct.2019.01.089
9. Bulut, M., Erklig, A., Alsaadi, M., Kchany, S. Effects of Stacking Sequence on Mechanical Properties of Hybrid Composites Reinforced with Carbon, Kevlar and S-Glass Fibers. Materials Testing. 2017. No. 59, no. 5. Pp. 472–79. http://dx.doi.org/10.3139/120.111022
10. Pothnis, J.R., Kalyanasundaram, D., Gururaja, S. Enhancement of Open Hole Tensile Strength Via Alignment of Carbon Nanotubes Infused in Glass Fiber – Epoxy – CNT Multi-Scale Composites. Composites Part a-Applied Science and Manufacturing. 2021. No. 140. Pp. 106–155. http://dx.doi.org/10.1016/j.compositesa.2020.106155
11. Alam, M.A., Sami, A., Mustapha, K.N. Embedded Connectors to Eliminate Debonding of Steel Plate for Optimal Shear Strengthening of RC Beam. Arabian Journal For Science And Engineering, 2017. No. 42, no. 9. Pp. 4053–68. http://dx.doi.org/10.1007/s13369-017-2572-5
12. Alam, M.A. Al Riyami, K. Shear Strengthening of Reinforced Concrete Beam Using Natural Fibre Reinforced Polymer Laminates. Construction and Building Materials. 2018. No. 162. Pp. 683–96. http://dx.doi.org/10.1016/j.conbuildmat.2017.12.011
13. Van de Weyenberg, I., Truong, T.C., Vangrimde, B., Verpoest, I. Improving the Properties of Ud Flax Fibre Reinforced Composites by Applying an Alkaline Fibre Treatment. Composites Part a-Applied Science and Manufacturing. 2006. No. 37, no. 9. Pp. 1368–76. http://dx.doi.org/10.1016/j.compositesa.2005.08.016
14. Goncalves, A.P.B., de Miranda, C.S., Guimaraes, D.H., de Oliveira, J.C., Cruz, A.M.F., Flbm da Silva, Luporini, S., Jose, N.M. Physicochemical, Mechanical and Morphologic Characterization of Purple Banana Fibers. Materials Research-Ibero-American Journal of Materials. 2015. No. 18. Pp. 205–209. http://dx.doi.org/10.1590/1516-1439.366414
15. El-Sabbagh, A., Steuernagel, L., Ziegmann, G. Characterisation of Flax Polypropylene Composites Using Ultrasonic Longitudinal Sound Wave Technique. Composites Part B-Engineering. 2013. No. 45, no. 1. Pp. 1164–72. http://dx.doi.org/10.1016/j.compositesb.2012.06.010

16. Renouard, S., Hano, C., Doussot, J., Blondeau, J.P., Laine, E. Characterization of Ultrasonic Impact on Coir, Flax and Hemp Fibers. Materials Letters. 2014. No. 129. Pp. 137–41. http://dx.doi.org/10.1016/j.matlet.2014.05.018
17. Prasad, V., Sekar, K., Varghese, S., Joseph, M.A. Evaluation of Interlaminar Fracture Toughness and Dynamic Mechanical Properties of Nano TiO2 Coated Flax Fibre Epoxy Composites. Polymer Testing. 2020. No. 91. Pp. 106784. http://dx.doi.org/10.1016/j.polymertesting.2020.106784
18. Ghaffar, S.H., Al-Kheetan, M., Ewens, P., Wang, T., Zhuang, J.D. Investigation of the Interfacial Bonding between Flax/Wool Twine and Various Cementitious Matrices in Mortar Composites. Construction and Building Materials. 2020. No. 239. Pp. 117833. http://dx.doi.org/10.1016/j.conbuildmat.2019.117833
19. El Jaouhari, A., Ben Jadi, S., El Guerraf, A., Bouabdallaoui, M., Aouzal, Z., Bazzaoui, E.A., Martins, J.I., Bazzaoui, M. Synthesis and Spectroscopic Characterization of Polypyrrole Ppy Coating on Flax Fibers and Its Behaviour toward Trimethylamine Vapor. Synthetic Metals. 2018. No. 245. Pp. 237–44. http://dx.doi.org/10.1016/j.synthmet.2018.09.014
20. Whitacre, R., Amiri, A., Ulven, C. The Effects of Corn Zein Protein Coupling Agent on Mechanical Properties of Flax Fiber Reinforced Composites. Industrial Crops and Products. 2015. No. 77. Pp. 232–38. http://dx.doi.org/10.1016/j.indcrop.2015.08.056
21. Kannan, T.G., Wu, C.M., Cheng, K.B. Influence of Laminate Lay-up, Hole Size and Coupling Agent on the Open Hole Tensile Properties of Flax Yarn Reinforced Polypropylene Laminates. Composites Part B-Engineering, 2014. No. 57. Pp. 80–85. http://dx.doi.org/10.1016/j.compositesb.2013.09.042
22. M.R., S., Siengchin, S., Parameswaranpillai, J., Jawaid, M., Pruncu, C.I., Khan, A. A comprehensive review of techniques for natural fibers as reinforcement in composites: Preparation, processing and characterization. Carbohydrate Polymers. 2019. 207. Pp. 108–121. DOI: 10.1016/j.carbpol.2018.11.083
23. Liu, Y., Lv, X., Bao, J., Xie, J., Tang, X., Che, J., Ma, Y., Tong, J. Characterization of silane treated and untreated natural cellulosic fibre from corn stalk waste as potential reinforcement in polymer composites. Carbohydrate Polymers. 2019. 218. Pp. 179–187. DOI: 10.1016/j.carbpol.2019.04.088
24. Balachandar, M., Vijaya Ramnath, B., Jagadeeshwar, P., Yokesh, R. Mechanical behaviour of Natural and Glass fiber reinforced with polymer matrix composite. Materials Today: Proceedings. 2019. 16. Pp. 1297–1303. DOI: 10.1016/j.matpr.20-19.05.227
25. Yoddumrong, P., Rodsin, K., Katawaethwarag, S. Seismic Strengthening of Low-Strength RC Concrete Columns Using Low-Cost Glass Fiber Reinforced Polymers (Gfrps). Case Studies in Construction Materials, 2020. No. 13. Pp. e00383. http://dx.doi.org/10.1016/j.cscm.2020.e00383

Information about authors:

Xiaolian Gai,
ORCID: https://orcid.org/0000-0002-0856-8560
E-mail: gaixiaolian@126.com

Dongpo He,
ORCID: https://orcid.org/0000-0003-2427-1086
E-mail: hdp@nefu.edu.cn

Hongguang Wang, *PhD*
ORCID: https://orcid.org/0000-0002-7620-614X
E-mail: wanghongguang@zoho.com

Received 04.01.2020. Approved after reviewing 08.10.2021. Accepted 09.10.2021.